**Accepted Article: Catalysis Today**

# The Role of Heterogeneous Catalysts in the Plasma-catalytic Ammonia Synthesis

Bhaskar S. Patil[1*], Nikolay Cherkasov[2], Nadadur Veeraraghavan Srinath[1], Juergen Lang[3], Alex O. Ibhadon[4], Qi Wang[1], Volker Hessel[1,5*]

[1] Micro Flow Chemistry and Process Technology, Eindhoven University of Technology, P. O. Box 513, 5600 MB Eindhoven, Netherlands

[2] School of Engineering, University of Warwick, Coventry, CV4 7AL

[3] Innovation Management, Verfahrenstechnik & Engineering, Evonik Industries AG, Rodenbacher Chaussee 4, 63457 Hanau-Wolfgang, Germany

[4] Department of Chemical Engineering, School of Chemical Engineering University of Hull, United Kingdom

[5] School of Chemical Engineering, The University of Adelaide, North Terrace Campus, Adelaide 5005, Australia

corresponding authors: volker.hessel@adelaide.edu.au and patilbhaskars@gmail.com; tel. +31(0)40 247 2973

## Abstract

Ammonia, being the second largest produced industrial chemical, is used as a raw material for many chemicals. Besides, there is a growing interest in the applications of ammonia as electrical energy storage chemical, as fuel, and in selective catalytic reduction of $NO_x$. These applications demand on-site distributed ammonia production under mild process conditions. In this paper, we investigated 16 different transition metal and oxide catalysts supported on γ-$Al_2O_3$ for plasma-catalytic ammonia production in a dielectric barrier discharge (DBD) reactor. This paper discusses the influence of the feed ratio ($N_2/H_2$), specific energy input, reaction temperature, metal loading, and gas flow rates on the yield and energy efficiency of ammonia production. The optimum $N_2/H_2$ feed flow ratio was either 1 or 2 depending on the catalyst – substantially above ammonia stoichiometry of 0.33. The concentration of ammonia formed was proportional to the specific energy input. Increasing the reaction temperature or decreasing gas flow rates resulted in a lower specific production due to ammonia decomposition. The most efficient catalysts were found to be 2 wt% $Rh/Al_2O_3$ among platinum-group metals and 5 wt% $Ni/Al_2O_3$ among transitional metals. With the 2 wt% Rh catalyst, 1.43 vol% ammonia was produced with an energy efficiency of 0.94 g $kWh^{-1}$. The observed behaviour was explained by a combination of gas phase and catalytic ammonia formation reactions with

plasma-activated nitrogen species. Plasma catalysts provide a synergetic effect by activation of hydrogen on the surface requiring lower-energy nitrogen species.

**KEYWORDS:** plasma catalysis, ammonia production, catalytic DBD reactor, supported transition metal oxides, energy efficiency, Haber-Bosch.

# 1. Introduction

Reactive nitrogen in the form of ammonia is an essential element for life on Earth;[1,2] it is the second-largest chemical compound produced and is essential for the global economy.[3] Ammonia is used as a starting material for the production of many chemical compounds such as fertilisers, explosives, and in many industries such as pulp and paper, refrigeration, pharmaceuticals, fibers and plastics, mining and metallurgy. Ammonia is produced on a major scale via the Haber-Bosch process at 450-600 $^{o}$C and 150-350 bar in the presence of a catalyst in megaton-scale centralised production facilities.[4] With the global population set to exceed 9 billion by 2050, ammonia is destined to become a focal point for intensification of agriculture and chemical industries.[56]

In addition to these well-established applications, ammonia attracts attention as an energy storage chemical,[7] fuel,[8] and as a reducing agent in selective catalytic reduction (SCR) of $NO_x$ produced by automobiles.[9] These applications demand distributed ammonia production under mild process conditions and on a smaller scale using electricity from renewable sources[1,10,11] because the Haber-Bosch process is not a viable option. Therefore, it is imperative to look for an alternative ammonia production process with zero $CO_2$ emissions, close to electricity generation, and at a point-of-use, as demanded by these emerging applications.[6,12,13]

Over the last century, several alternative approaches have been developed for $CO_2$-free ammonia synthesis under mild operating conditions such as electron-driven electro- and photo-catalysis, homogeneous and enzyme catalysis.[14] Among these alternative approaches, non-thermal plasma (NTP) generated by renewable electricity is an appealing option for small scale and distributed production.[15–19] NTPs are characterised by an excessively high electron temperature, while the bulk of the gas remains at a mild temperature. These non-equilibrium properties enable thermodynamically unfavourable chemical reactions under mild conditions such as atmospheric pressure and low temperature.[20,21] In addition, NTP offers an opportunity to use catalysts to benefit surface reactions and increased selectivity towards the desired product.[22–24] Such a combination of NTP with a catalyst (plasma catalysis) often yields synergetic effects with the efficiency of the combined system exceeding that of the constituent parts.[23–27]

The ease of catalyst screening and simplicity of operation motivated many plasma catalysis studies for ammonia synthesis in a dielectric barrier discharge (DBD) reactor.[28–31] Most of the reported literature studies use relatively inert (or ferroelectric) materials conventionally considered as catalyst support.[31–35] These materials, nevertheless, show significant improvements in nitrogen fixation due to their effect on the

plasma formation.[31,36] Mizushima et al.[37] showed that loading active metals on the support can yield higher ammonia concentration and can also improve the energy yield. The ammonia yield was reported to increase in the following order Ru > Ni > Pt > Fe > only $Al_2O_3$.[37] Recently, Peng et al.[38] used 10% Ru+Cs/MgO catalyst and Hong et al.[39] reported ammonia over a functional carbon-coated catalyst. Iwamoto et al.[40] and Mehata et al.[41] attempted to explain the differences in reactivity between various metals and evaluated it through DFT calculations and microkinetic modelling.

Even though the plasma-assisted ammonia syntheses have long been investigated using various plasma catalysts, the nature of the support-catalyst effect is largely unknown; the performance of different supported catalysts and reasons of their synergy is scarcely available. Moreover, no detailed studies exist that explain the influence of the feed composition, temperature and metal loading. In this paper, we aim to study the role of active component in heterogeneously-catalysed plasma-catalytic ammonia synthesis. To achieve this and distinguish between the electrical and curvature effects of various materials, we used supported catalysts with low metal loading deposited on the same particles of γ-alumina.

## 2. Experimental section

Pelletized γ-$Al_2O_3$ was purchased from Mateck GMBH, crushed, and sieved into a 250-350 µm fraction. The particle size fraction was selected to have an optimum performance in the reactor, low-pressure drop, and high product yield.[31,36] The supported catalysts were prepared using wet impregnation and calcined at 450 $^oC$, more details are in the Supplementary S1. The catalysts obtained are referred by the weight loading of the active metal and its type, for example, 2 Ru for 2 wt% Ru/ γ-$Al_2O_3$.

Fig. 1 shows a one-sided DBD plasma-catalytic reactor. The reactor has an axial high-voltage electrode (a stainless-steel rod, 6 mm outer diameter) and a ground electrode (a stainless mesh wrapped around the quartz reactor body, 10 mm inner diameter). The catalysts are placed directly in the plasma discharge zone of the DBD reactor (100 mm) and kept in-place with quartz wool plugs (Carl Roth GmbH) positioned outside the catalyst bed.[31,36] The reactor was positioned in a tube furnace to heat only the catalyst zone while keeping the reactor ends outside of the furnace (Supplementary S2).

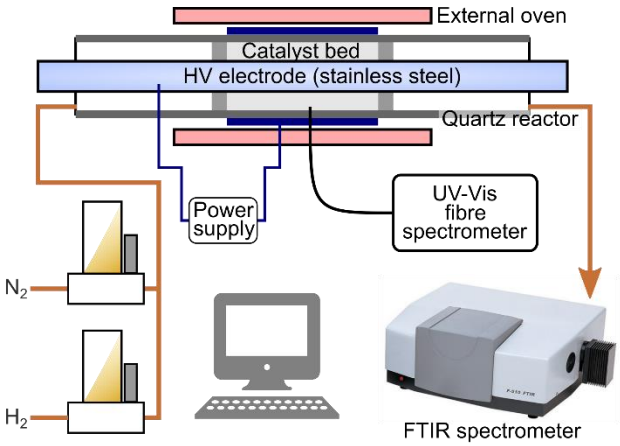

**Fig. 1. A scheme of the experimental set-up with a one-sided dielectric barrier discharge (DBD) plasma reactor.**

The reactants, $N_2$ and $H_2$ gases (Linde, 99.9%), controlled with mass-flow controllers were fed into the reactor and the voltage was applied at a frequency of 21 kHz and the pulse width 25 μs. The flow rates of gases are reported under the normal temperature and pressure conditions. The product gases were analysed with a Fourier transform infrared spectrophotometer (Shimadzu IRTracer-100) in a Specac gas cell with KBr windows. The only product detected was ammonia and its concentration was quantified at the wavelength of 965 $cm^{-1}$ calibrated with a series of reference gas mixtures.

All the voltage and current signals were logged with a 4 channel PicoScope® 3000 oscilloscope. The applied voltage (measured with a Tektronix P6015A probe), the voltage across a 100 nF capacitor, and operational frequency allowed estimating power consumed by the DBD plasma reactor using the method reported by Manley.[42] The total power ($p_{tot}$), specific energy input (*SEI*), and the energy consumption per mole of ammonia produced (*E*) were calculated using equations (1-3), where *f* is the applied voltage frequency, *V* is the applied voltage, $C_p$ - the capacitor value, $Q_{gas}$ is the total volumetric gas flow rate, $C_{NH3}$ is the concentration of ammonia produced.

$$p_{tot} = f\, C_p \int_{one\ cycle} V(t)dt, \qquad (1)$$

$$SEI = {}^{p_{tot}}/_{Q_{gas}}, \qquad (2)$$

$$E = {}^{p_{tot}}/_{Q_{gas}\, C_{NH3}}, \qquad (3)$$

Prior to every experiment, the catalyst was in situ reduced at a fixed energy input of 42 W in a flow of hydrogen of 0.2 L $min^{-1}$ for 30 min. All experiments were performed twice with reproducibility above ±5%. The temperature of the plasma region and the outgoing gas were monitored with thermocouples and an infrared camera. The highest temperature of the packed bed and the central electrode was found to be 420 oC, while the gas outlet temperature was always below 26 oC. Blank experiments without plasma, but thermal heating to 400 oC, showed no $NH_3$ formation with all the catalysts. Therefore, all $NH_3$ detected was formed only during plasma or plasma-catalytic processes.

The light emitted by the plasma discharge was collected with an optical fibre and analysed with an HR2000+ spectrometer at 10 s integration time and 0.2 nm $pixel^{-1}$ resolution. Confocal collection optics improved the signal-to-noise ratio and a spatial resolution to about 1 mm.

All the catalysts were characterized before and after plasma exposure. To investigate the effect of the plasma discharge on the catalyst morphology, the catalysts were studied with nitrogen physisorption and scanning electron microscopy coupled with energy-dispersive spectroscopy (SEM-EDX). The state of the supported metal and metal oxide particles was analysed with transmission electron microscopy (TEM), and the oxidation state – with temperature-programmed reduction (TPR). The experimental details and information obtained are provided in Supplementary S3.

# 3. Results and discussion

## 3.1. Oxidation state of the catalyst and feed ratio optimisation

Before carrying out plasma ammonia synthesis, we studied the effect of hydrogen plasma treatment on the catalysts. The results of the temperature-programmed reduction experiments of the catalysts before and after the plasma exposure are shown in Supplementary S3, summarised in Table 1.

**Table 1. The fraction of the metal oxide to metal reduction in a hydrogen plasma.**

| Catalyst | Reduction (%) |
|---|---|
| 2 Pt | 98.6 |
| 2 Pd | 100 |
| 2 Rh | 99.0 |
| 2 Ru | 100 |
| 10 Ni | 57.7 |
| 10 Fe | 52.4 |
| 10 W | 50.0 |
| 10 Mo | 20.4 |
| 10 Mn | 46.7 |
| 5 Co | 75.8 |
| 5 Cu | 84.5 |
| 5 V | 23.6 |

The platinum-group catalysts were completely or mostly reduced by the $H_2$ plasma. For example, a low-temperature reduction peak below 200 $^oC$ in the 2 Pt catalyst disappeared after plasma treatment. The reduction of active metals was likely attained thermally as well because the catalyst temperature reached 420 $^oC$ during the plasma treatment; however, other plasma-specific reduction mechanisms could have been also present.[43] Most other metal oxides (Table 1) were also significantly reduced in plasma, in agreement with literature.[44–52] The oxides of W, Mo, V, and Mn were only partially reduced because they require a temperature of above at 800 $^oC$ in $H_2$ for complete reduction. The Ni, Cu, Fe, Co catalysts likely contained metal sites on their surface while the bulk reduction was limited by diffusion limitations of hydrogen through the oxides. The catalyst characterisation before and after the plasma treatment (Supplementary S3) shows no significant changes.

The characterisation (Supplementary S3) also shows surface area and porosity for the catalysts were close likely because they were determined by the alumina support. A relatively low loading of active component onto the same support ensures similar *bulk* properties of the catalysts and allows us to decouple the bulk electronic and electrical properties from the surface chemistry. The bulk properties determined by the support were similar, while the surface properties determined by the active material were varied in the current study to study the effect of surface chemistry.

Starting with the catalysts reduced ex-situ at 800 °C, we optimized the volumetric feed $N_2/H_2$ ratio in the range of 4 to 0.33 at a fixed total flow rate and a constant power input. Fig. 2 shows the effect of the feed ratio on the ammonia concentration for selected catalysts, all catalysts are shown in Supplementary S4. The catalysts significantly affected the ammonia concentration demonstrating an effect on the plasma reaction – the optimum feed ratio (the $N_2/H_2$ ratio resulting in the highest ammonia concentration) was either 1 or 2.

The reactor without any catalyst showed the optimum feed ratio of 1. The reactor filled only with the catalyst support ($\gamma$-$Al_2O_3$) showed the same optimum feed ratio, but a significantly higher concentration of ammonia. The optimum feed ratio varied for the best performing platinum-group catalysts. The 2 Rh, 2 Ru, and 2 Pt catalysts showed the optimum ratio of 2, while the less effective 2 Pd catalyst had the optimum ratio of 1 (Fig. 2A).

The optimum feed ratio for other transition metal catalysts was also either 1 or 2. The catalysts such as 10 Ni, 10 Co and 10 Mo increased the concentration of ammonia obtained compared to the catalyst support and showed the optimum feed ratio of 2 (Fig. 2B). The 10 W catalyst suppressed the ammonia formation compared to the support, while the 10 Mn and 10 Fe catalysts showed a lower ammonia formation even compared to the empty reactor. We used the feed ratio of either 1 or 2 in the subsequent experiments – the optimum ratio for each catalyst. Such changes in the feed ratio, however, had a minor effect because the ammonia concentration changed by less than 4 %

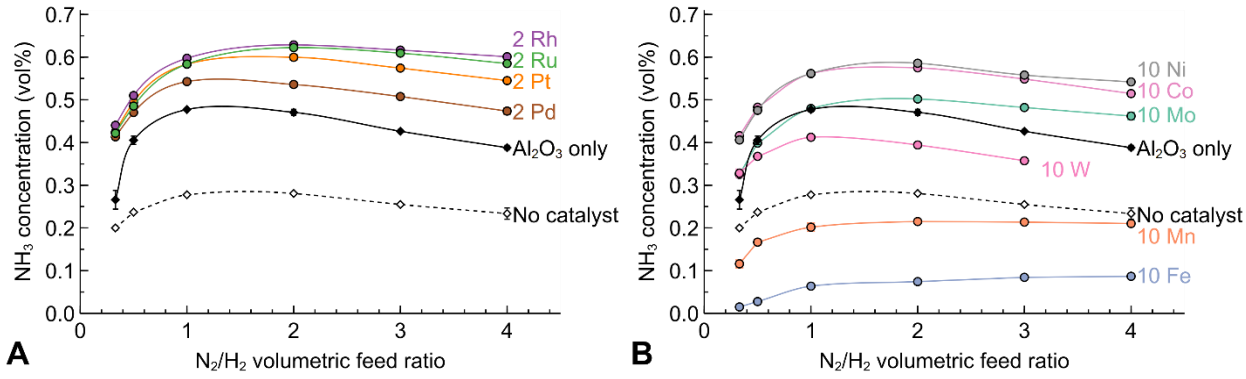


**Fig. 2. The effect of the $N_2$ to $H_2$ volumetric feed ratio on ammonia formation in a plasma-catalytic reactor packed with various alumina-supported catalysts at the total flow rate of 0.18 L $min^{-1}$.**

The optimum $N_2/H_2$ feed ratio for the plasma-catalytic (1 – 2) and thermal (0.33) reactions are notably different – it indicates various reaction mechanisms – as also reported by: Plasma Chem Plasma Proc V20, 511, 2000; Plasma Process Polymer V14, e1600157, 2017; J Phys D: Applied Physics, V53, 014008 (2020). The required high $N_2$ concentration may be understood considering that ammonia formation is determined by activation of nitrogen molecules in the plasma because the nitrogen dissociation energy of 9.76 eV is substantially higher than that of hydrogen ( 4.48 eV).[53,54] The increasing $N_2$ concentration likely leads to a higher probability of its activation, and in turn higher ammonia formation. Increasing the $N_2$

concentration (or the feed ratio) above the optimum point likely decreases the availability of hydrogen for the ammonia formation.

### 3.2. Effect of the plasma energy input and catalyst loading

The feed ratio study already gives strong indications that plasma ammonia synthesis has a reaction mechanism substantially different from that of the thermal reaction. Therefore, we studied the effect of plasma energy input on ammonia production (Fig. 3 for the selected catalysts, all catalysts are presented in Supplementary S5). The results demonstrate that catalysts play a major role in plasma ammonia synthesis. At a comparable energy input, the 2 Ru catalyst showed almost 30 % higher ammonia concentration compared to the alumina catalyst support. The concentration of ammonia formed was proportional to the energy input and the slopes for the empty reactor was the lowest.

The formation of ammonia without any catalyst shows that ammonia could be formed in the gas-phase reaction. In the presence of catalysts, the ammonia formation increases further indicating either the presence of surface (heterogeneous) ammonia formation or enhancement of gas-phase ammonia formation by the catalysts. The plasma enhancement by the catalysts is a possibility discussed further and strongly suggested by the enhanced ammonia formation by the alumina support – a rather chemically inert material that unlikely to show a significant surface reaction. A further increase in ammonia formation by the addition of several percent of active metal (2 Ru and 5 Co catalysts) is likely caused by the surface reactions of the excited species. The reason is that the bulk properties of the catalysts stay similar to that of the support and a notable change in plasma properties is unlikely. The effects of catalysts on plasma are discussed further.

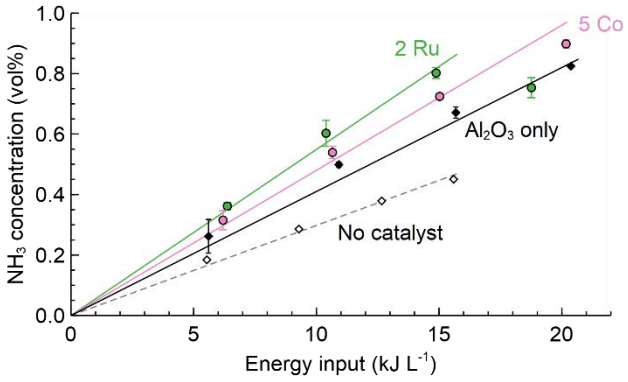


**Fig. 3. Ammonia concentration obtained in a plasma-catalytic reactor as a function of specific plasma energy input for selected cases at a fixed linear gas velocity.**

For most of the catalysts studied, ammonia concentration was proportional to the plasma input as shown in Fig. 3 for the 5 Co catalyst. In some cases, however, an increase in the input energy beyond a certain threshold had either a minor or even a detrimental effect on ammonia formation. For the 2 Ru catalyst, for example, increasing energy input beyond 15 kJ $L^{-1}$ did not increase ammonia formation likely because of thermal decomposition of ammonia at a higher temperature. Importantly, for a lower plasma energy input,

the concentration of ammonia formed over the 2 Ru catalyst was also proportional to the plasma energy. Therefore, the effect of catalysts on plasma ammonia formation can be characterised by a single value of plasma ammonia formation efficiency – the slope of the linear part of the plot.

Table 2 compares the plasma ammonia formation efficiency for selected catalysts with the full table presented in Supplementary S5. First of all, the data show that doubling the metal loading in the Ni, Fe, Co, or Mo catalysts has a negligible effect on the plasma ammonia formation, resulting in the same plasma efficiency. Roland et al.[55] and Zhang et al.[56] showed that the electrical discharge does not penetrate into the pores smaller than about 0.8 μm. Hence, discharges must be primarily formed between the 300 μm catalyst support particles resulting in contribution mainly from the external catalyst surface.

**Table 2. Comparison of plasma ammonia formation efficiency (k) – the slope of plots in Fig. 3 for selected catalysts at the total flow rate of 0.18 L min$^{-1}$.**

| Catalyst | $k$ ($nL_{NH3}$ $J^{-1}$) |
|---|---|
| 2 Ru | 554 |
| 2 Rh | 514 |
| 10 Ni | 506 |
| 5 Ni | 495 |
| 2 Pt | 491 |
| 10 Co | 484 |
| 10 Fe | 484 |
| 2 Pd | 483 |
| 5 Co | 468 |
| 5 Mo | 446 |
| 10 Mo | 445 |
| $Al_2O_3$ | 422 |
| No catalyst | 298 |
| 10 Mn | 273 |

It is interesting to compare the catalyst activity sequence in thermal ammonia formation and in plasma. In the conventional Haber-Bosch process where the rate-limiting step is dissociative adsorption of nitrogen molecules, the following catalyst sequence is observed: Ru > Rh > Fe > Co > Mo > Ni ≫ Pd.[57,58] In case of the plasma catalysis studied, the activity sequence is different, being Ru > Rh > Ni > Co > Fe > Pd ≫ Mo. The most notable differences in the positions of Pd and Mo suggest that nitrogen activation *on the catalyst surface* is not the rate-limiting stage in plasma-assisted ammonia synthesis. This is further supported by the absence of ammonia formation without plasma.

The observed catalyst sequence can be compared to the binding energy of molecular hydrogen which is Pt < Ru < Pd < Ni < Fe < Mo.[59] This sequence is close to that observed in plasma-catalytic ammonia synthesis with a few notable exceptions, such as Pd, which was found to be less active compared to the Fe catalyst. The differences may be explained by the effect of the active metal on plasma generation.[36]

Overall, the data indicate that in plasma-catalytic ammonia synthesis, nitrogen is predominately activated in plasma and reacts with hydrogen species activated on the surface of heterogeneous catalysts. However, there is a notable formation of ammonia even in the blank experiments and on the alumina catalyst indicating that a parallel gas-phase (homogeneous) ammonia formation also takes place.

### 3.3. Effect of flow rate and the reaction temperature

At the next step, we studied the effect of gas feed flow rate on the plasma-catalytic ammonia formation for the most efficient base-metal 5 Ni catalyst and the platinum-group 2 Rh catalyst. The 2 Rh catalyst has an activity similar to that of Ru but does not show a pronounced ammonia decomposition at the increased plasma energy input.

Fig. 4 demonstrates that the behaviour of both catalysts was comparable – the ammonia formation was proportional to the plasma energy input up to certain energy. At high gas flow rates of 1 and 0.6 L $min^{-1}$, the slope in the ammonia concentration was independent of the flow rate corresponding to the intrinsic catalyst activity which was higher for Rh compared to Ni. A decreasing gas flow rate, however, resulted in a deviation from the observed trend and a lower ammonia generation efficiency possibly due to the thermal decomposition of ammonia.

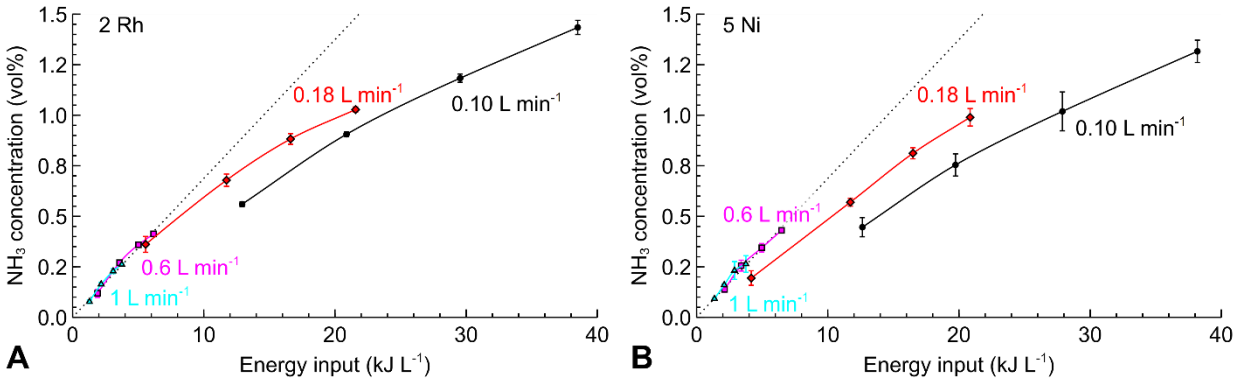


**Fig. 4. The effect of the total gas flow rate ($N_2/H_2$ = 2 vol.) on ammonia plasma formation over the (A) 2 Rh and (B) 5 Ni catalysts in a plasma-catalytic reactor.**

The effect of the reaction temperature (measured externally at the reactor wall) on plasma-catalytic ammonia formation was studied by heating the plasma reactor externally (with a furnace), the performance of selected catalysts shown in Fig. 5. The full plot for all the catalysts studied is presented in the Supplementary Information S6, Fig. S19. Generally, the concentration of ammonia increased slightly with temperature followed by a sharp decline. The optimum temperature (temperature corresponding to the highest ammonia concentration) significantly depended on the catalyst. The empty reactor showed a consistent small increase in ammonia concentration with reaction temperature, while the reactor filled with the alumina support showed a small decline after 300 $^oC$ – similar for the 2 Rh and 10 Ni catalysts. The 2 Ru and 10 Mn catalysts demonstrated a continuous decline in ammonia formation with temperature.

Therefore, the experiments confirm that the declining ammonia concentration at higher plasma energy can be explained by thermal ammonia decomposition.

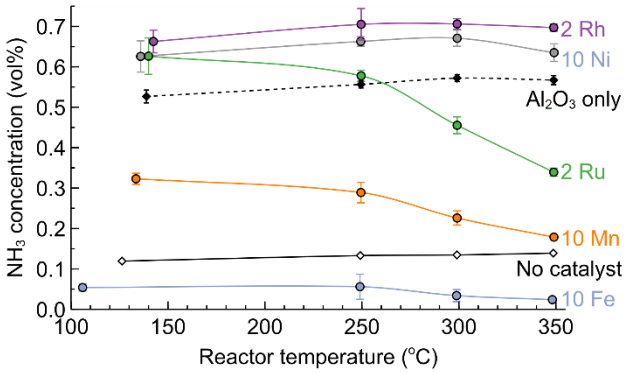


**Fig. 5. Ammonia concentration obtained in a plasma-catalytic reactor concentration as a function of the reaction temperature (measured externally at the reactor wall) at a fixed input voltage and total gas feed flow rate of 0.18 L min$^{-1}$.**

The observed phenomena of declining ammonia concentration with temperature can be explained with Le Chatelier's principle. Ammonia synthesis is an exothermic reaction; hence, an increasing temperature shifts equilibrium towards the starting materials. In the conventional Haber-Bosch thermal ammonia synthesis, a high reaction temperature (400-500 $^{o}$C) is required to increase the reaction rates, while the shift in the equilibrium position is counterbalanced by high pressure (>100 bar).[30] Similarly, the observed decrease in ammonia concentration with temperature (Fig. 5), might be explained by thermodynamic effects of shifting equilibrium position. In this case, we can expect, however, reaching a certain equilibrium-limited line independent of the catalysts studied which was not observed experimentally. Therefore, the effect of reaction temperature might have been caused by local equilibria in the plasma vicinity. A higher reaction temperature may also result in lower hydrogen adsorption on the catalyst surface, thus reducing the probability of the heterogeneous reaction with activated nitrogen species.

The experimental data shows that the reactor temperature should be maintained in the range of 250 - 300 $^{o}$C for most catalysts in order to achieve the highest concentration of $NH_3$. The concentration increases at a such temperature, however, is small and external heating may be economically unjustified. On the other hand, the increasing plasma energy input raises the temperature and a reactor cooling should be employed to keep the temperature below 300 $^{o}$C.

### 3.4. Effect of catalyst on the plasma characteristics

The previous sections showed that the catalysts affect ammonia formation significantly via surface reaction. The catalysts, however, may also affect the plasma formation as observed in the nitrogen oxidation reaction.[36] In a DBD reactor packed with γ-$Al_2O_3$, filamentary micro discharges are predominant with

considerably higher energy electrons compared to Townsend-like discharges.[60] The filamentary discharges are more efficient in plasma ammonia formation, and the ammonia formation efficiency may be increased by if the plasma energy is directed exclusively to the filamentary discharges.

Fig. 6 shows the voltage-current plots for several catalysts studied. Here, the number and intensity of the discharges can be assessed by the spikes in the current and voltage. The data show that the intensity and the number of filaments increase in the reactor filled with the alumina support compared to the empty reactor. This observation indicates that a higher ammonia formation efficiency observed in Fig. 3 is likely caused by the enhanced plasma formation.

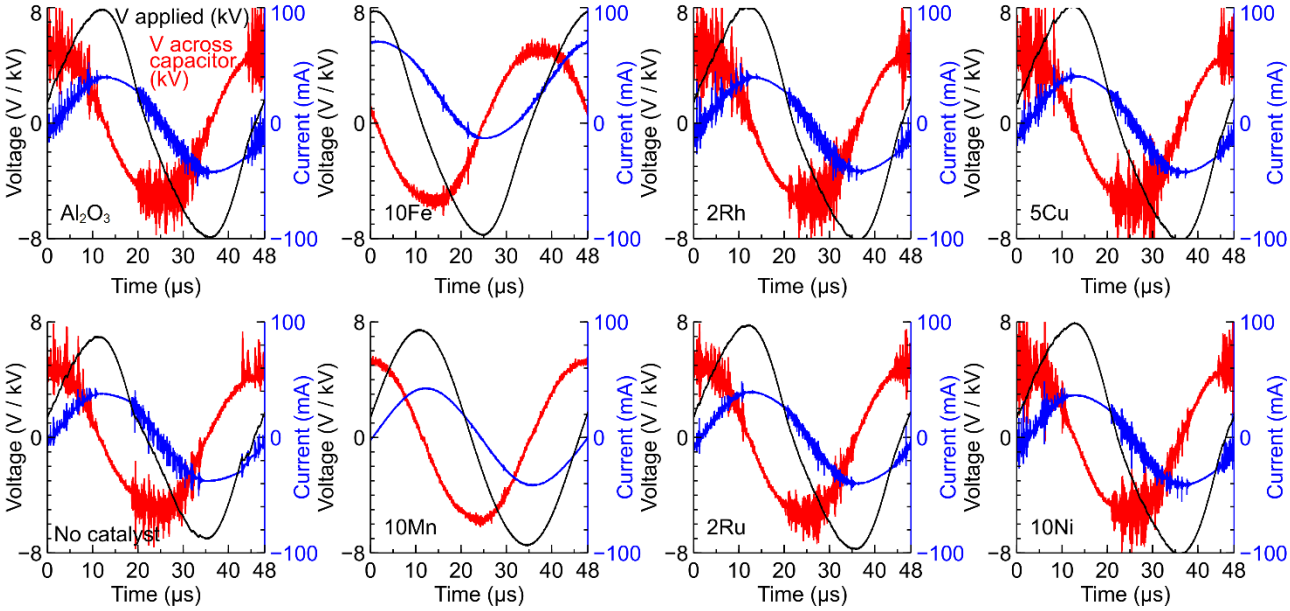


**Fig. 6. Applied voltage (black), voltage across measuring capacitor (red), and current (blue) observed in a plasma-catalytic reactor packed with a range of alumina-supported catalysts, catalyst support (alumina), and without any materials.**

The metals added on the support resulted in a notable effect on plasma formation. The most obvious difference is seen when comparing the reactor filled with $Al_2O_3$, 10 Mn, and 10 Fe catalysts. The latter two catalysts show a dramatic decrease in the discharges – almost complete absence of spikes in current indicates a non-filamentary Townsend-like discharge. The best-performing platinum-group catalysts show plasma discharge with characteristic filamentary discharges evidenced by a large number of high-intensity spikes.

The number of plasma discharges alone does not seem to be a determining factor in plasma ammonia formation because the 2 Ru catalysts showed notably weaker discharges compared to the 2 Rh catalyst despite their comparable ammonia formation efficiency. On the contrary, 5 Cu catalyst showed more intensive discharges compared to the 10 Ni catalyst while the latter was forming significantly more ammonia.

Therefore, the data show that the supported active metals affect the plasma generation. The inefficient plasma catalysts such as 10 Fe or 10 Mn notably suppress plasma generation. More efficient catalysts, however, do not show a correlation with the plasma generation indicating a significant effect of surface catalyst phenomena onto the ammonia plasma synthesis.

### 3.5. Energy Efficiency for plasma-catalytic ammonia synthesis

Table 3 shows, in effect, the energy efficiency of plasma-catalytic process forming ammonia in the current studies and the literature sources. The lowest energy consumption of 32 MJ $mol^{-1}$ at an ammonia concentration of 0.3 vol% was achieved in this study for the 2 % Rh catalyst at a total gas flow rate of 1 L $min^{-1}$, which corresponds to 1.9 g of ammonia per kWh. Increasing ammonia concentration to 1.43 vol% required almost doubling the energy input to 65 MJ $mol^{-1}$ due to thermal decomposition of ammonia. The energy efficiency of plasma ammonia realized in this study is amongst the highest that are reported in the literature. However, it is worth noting that these values are far from the benchmark Haber-Bosch process, which consumes only 0.5 MJ $mol^{-1}$ for the entire process including energy-intensive $H_2$ production by steam reforming. The Haber-Bosch also operates under a higher per pass $N_2$ conversion of 10-15%. Nevertheless, the plasma synthetic process operating under ambient pressure and requiring only a source of electricity is a promising alternative for smaller-scale decentralized production where large capital investment into Haber-Bosch plant cannot be justified.

**Table 3. Comparison of the energy consumption required for plasma ammonia synthesis in dielectric-barrier discharge (DBD) reactors.**

| Reactor | Experimental conditions | Feed gases | Products and concentration | Energy (MJ/mol) | Ref. |
|---|---|---|---|---|---|
| Packed DBD reactor | MgO + glass beads. $Q_{total}$[a] = 40 mL $min^{-1}$ (10 mL $min^{-1}$ Ar) | $N_2$ + $H_2$ + Ar | $NH_3$ at 0.57 vol%, per pass $H_2$ conversion of 4.2 % | 576 | 33 |
| Packed DBD reactor | Ferroelectric material. $Q_{total}$[a] = 11.5 mL $min^{-1}$ at $N_2/H_2$ = 1/3 | $N_2$ + $H_2$ | $NH_3$ at 3.3 vol%, per pass of $N_2$ conversion of 7% | 408 | 35 |
| Packed DBD reactor | Functional carbon coatings on α-$Al_2O_3$. $Q_{total}$[a] = 50 mL $min^{-1}$, $N_2/H_2$=1/3. | $N_2$ + $H_2$ | $NH_3$ at 1.2 vol%. | 350 | 39 |
| DBD reactor with catalytic membrane | Various active metals supported on the alumina membrane. $Q_{total}$[a] = 30 mL $min^{-1}$, $N_2/H_2$=1/3 | $N_2$ + $H_2$ | $NH_3$ at 1.2 vol% (no $N_2H_4$ detected), per pass $N_2$ conversion of 2.4 % | 250 | 37 |

| | | | | | |
|---|---|---|---|---|---|
| DBD reactor with catalytic membrane | $Q_{total}$[a] = 40 mL min$^{-1}$, $N_2/H_2$ = 1/3 | $N_2 + H_2$ | $NH_3$ at 2.0 vol% (no $N_2H_4$ detected), per pass $N_2$ conversion of 4.0 % | 192 | [30] |
| Packed DBD reactor | Ferroelectric material (PZT and BaTiO3). $Q_{total}$[a] = 38.3 mL min$^{-1}$, $N_2/H_2$ = 1/1. | $N_2 + H_2$ | $NH_3$ at 2.8 vol%, per pass $N_2$ conversion of 2.7% | 136 | [34] |
| Micro-gap DBD reactor | $Q_{total}$[a] = 500 mL min$^{-1.}$ | $CH_4 + N_2$ | Products are $H_2$ and $NH_3$ (0.8 vol%) | 109 | [29] |
| Packed DBD reactor | 2 wt% Rh/γ -$Al_2O_3$. $Q_{total}$[a] = 100 mL min$^{-1}$, $N_2/H_2$=2/1 | $N_2 + H_2$ | $NH_3$ at 1.4 vol%, per pass $N_2$ conversion of 1.1% | 65 | This work |
| Packed DBD reactor | γ -$Al_2O_3$. $Q_{total}$[a] = 400 mL min$^{-1.}$ | $N_2+H_2$ | $NH_3$ at 0.35 vol%, per pass $N_2$ conversion of 0.26% | 52 | [31] |
| Packed DBD reactor | 2 wt% Rh/γ -$Al_2O_3$. $Q_{total}$[a] = 1000 mL min$^{-1}$, $N_2/H_2$=2/1. | $N_2 + H_2$ | $NH_3$ at 0.27 vol%, per pass $N_2$ conversion of 0.4% | 32 | This Work |
| Packed DBD reactor | 10 wt% Ru/MgO with Cs promoter. $Q_{total}$[a] = 4000 mL min$^{-1}$, $N_2/H_2$=3/1. | $N_2 + H_2$ | $NH_3$ at 3.7 vol% | 27 | [38] |
| Packed DBD reactor | Ru(2)-Mg(5)/ γ -$Al_2O_3$, $N_2/H_2$=4/1, at temperature <250 °C | $N_2 + H_2$ | NH3 at 1500 PPM at 36 g/kWh | 1.7 | Plasma Process Polymer V14 (6), e1600157, 2017 |

### 3.6. Spectroscopic study of the plasma-catalytic ammonia formation mechanism: rewrite this section!

Fig. 7 shows optical emission spectra of the plasma generated in the plasma-catalytic reactors for selected catalysts. The emission lines observed correspond to electron transitions in the neutral $N_2$ molecules, ionised $N_2$ molecules, and ionised N atoms.[61–63] The shape of the lines with strong peaks and tails towards the lower wavelengths is caused by the combination of rotational and vibrational excitation along with the electronic transitions.[64] No emission from the $H_2$ species was observed because only a few low-intensity lines could be observed in the spectral region studied. The broad line at 337 nm indicates the presence of excited NH* radicals with the emission line of 336.0 nm. The emission lines were observed for all the cases studied: when no catalyst was placed into the reactor, in the presence of only the alumina support and for active Rh or inactive Mn catalysts.

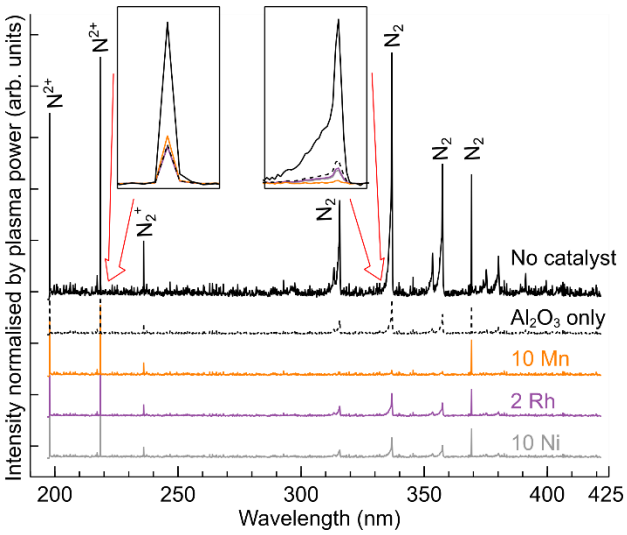


**Fig. 7. Optical emission spectra observed in a plasma-catalytic for selected cases.**

The emission intensity normalised by the input plasma power, however, was dramatically different as shown in the zoomed-in lines of the $N^{2+}$ and $N_2$ $A^3\prod$ to $X^3\sum$ transitions, Fig. 7. The highest emission intensity was observed when no catalyst was placed into the reactor. This observation may seem surprising; however, it can be easily explained by an extensive factor – signal accumulation from the whole reactor volume compared to only a narrow region near the reactor wall in case of the packed reactor. The light emitted from within the reactor could not penetrate through the packed material.

Comparing the emission lines from the packed reactors, the most intensive $N^{2+}$ emission line was observed for the least active 10 Mn catalyst while the other materials showed a similar, about 30% lower, emission intensity. The lines corresponding to the excited $N_2$ species at 337 nm were notably different. The most intensive emission was observed for the catalyst support, the most active 2 Rh and 10 Ni catalysts showed a slightly lower intensity, while the inactive 10 Mn catalyst showed minor emission.

Fig. 8 summarises the observed data on ammonia plasma-catalytic formation. (The mechanistic aspects of each reaction stage is provided in reviews.[65,66]) On the application of an electric potential to a packed DBD reactor, plasma generates high-energy electrons. Plasma formation, however, is affected by the catalyst properties.[36] Even in the case of supported catalysts studied that contain only 5-10 wt% of active material, the effect of a catalyst on plasma cannot be discarded as demonstrated by the 10 Mn and 10 Fe catalysts. Those catalysts notably inhibit plasma formation and generate low-energy Townsend discharges compared to filamentous discharges observed for other catalysts.

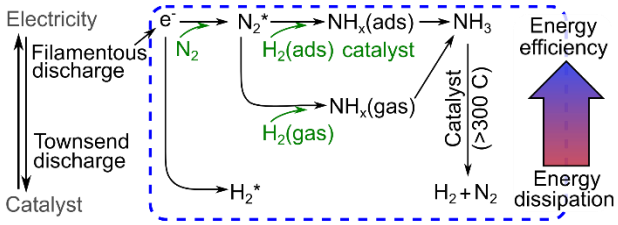


**Fig. 8. Scheme of the key processes occurring during plasma-catalytic ammonia formation.**

The high-energy electrons collide with the molecules of the gas phase – notably $H_2$ and $N_2$. Excitation of $H_2$ molecules results in eventual thermal energy dissipation via molecular collisions and does not produce ammonia due to insufficient energy for $N_2$ activation. The decrease in nitrogen activation with the addition of hydrogen had also been observed in microwave studies.[67] Hence, the $N_2/H_2$ initial ratio in the plasma processes should be kept well above the stoichiometric ratio of 0.33 – at 1 or 2 to minimise energy dissipation via $H_2$ collisions.

The collision of $N_2$ molecules with high-energy electrons can lead to excitation, ionisation or even dissociation. The excited $N_2$ species have two parallel reaction routes of (i) homogeneous reaction with $H_2$ molecules or (ii) heterogeneous reaction with $H_2$ adsorbed onto the catalyst surface. In both cases, the resulting $NH_x$ excited molecules undergo further reactions with $H_2$ to obtain the desired $NH_3$ products.[68,69] In the presence of the catalysts, $NH_3$ molecules can be adsorbed onto the catalyst surface and decompose thermally if the reaction temperature exceeds a threshold value of about 250-300 $^oC$ (Fig. 5).

## 4. Conclusions

A range of catalysts have been systematically screened for plasma-assisted ammonia synthesis in a packed dielectric barrier discharge (DBD) reactor at atmospheric pressure. The efficiency of plasma-catalytic ammonia formation depends significantly on the initial $N_2/H_2$ feed ratio which should be in the range of 1-2 for maximum ammonia production. The gas feed ratio is substantially above the stoichiometric ratio of 0.33 due to the possible energy dissipation by activation of hydrogen. The most active plasma catalysts (2 wt% $Rh/Al_2O_3$ and 10 wt% $Ni/Al_2O_3$) showed a significant synergetic increase in the ammonia concentration by 95% and 85%, respectively, compared to the empty plasma reactor or by 32% and 24% compared to the $\gamma$-$Al_2O_3$ catalyst support.

Increasing the metal loading showed virtually no effect on the ammonia produced, which indicates that the formation of microdischarges takes place in the inter-particle pores rendering the catalyst pores inaccessible for nitrogen fixation. The effect of temperature on the performance of all the catalysts was also investigated. The results show that the concentration of ammonia decreases at higher temperatures, indicating an increased rate of ammonia decomposition. For the experimental conditions employed in this study, varying the flow rate by almost an order of magnitude revealed a minor dependence on the residence time in the reactor likely because the plasma processes were much faster than the residence time.

The synergetic plasma-catalyst effect observed is associated with the reactions between the nitrogen molecules activated in plasma with hydrogen molecules activated over the catalyst surface. The surface reaction takes place in parallel with the gas-phase reaction between the plasma-activated nitrogen species and hydrogen molecules. However, no non-plasma ammonia formation was observed under the conditions studied. On the contrary, thermal decomposition of the ammonia was noticed for most catalysts, notably, 2 wt% Ru/γ-$Al_2O_3$. Due to the possibility of thermal decomposition, the plasma energy efficiency of ammonia formation was constant up to certain energy input and then declined. The threshold plasma energy corresponded to the gas temperature in the plasma reactor sufficient for ammonia thermal catalytic decomposition. The catalysts also influenced the formation of plasma and even substantially suppressed it as observed for the 10 wt% $Mn/Al_2O_3$ and 10 wt% $Fe/Al_2O_3$ catalysts.

At the optimum conditions, the ammonia concentration of 1.43 vol% was achieved in this study in a single-pass ambient pressure experiment over the 2 wt% Rh/γ-$Al_2O_3$. The corresponding ammonia formation energy efficiency was 65 MJ $mol^{-1}$ and the per pass hydrogen conversion of 6.4%. This result is among the best performances reported in the literature on plasma catalysis and shows the way for the distributed in-situ manufacturing of small amounts of ammonia. Replace this with new analysis!

**ACKNOWLEDGEMENT**

This research is funded by the EU project MAPSYN: Microwave, Acoustic and Plasma SYNtheses, under the grant agreement no. CP-IP 309376 of the European Community's Seventh Framework Program.

**SUPPLEMENTARY DATA**

Supplementary Data associated with this paper can be found in the online version of the paper and contains the following information: S1. Catalyst wet impregnation procedure; S2. Detailed scheme of the reactor; S3. Catalyst characterization data; S4. Effect of the gas feed ratio on the plasma-catalytic synthesis of ammonia; S5. Effect of the plasma energy input and catalyst loading; S6. Effect of the reaction temperature on the ammonia plasma-catalytic formation. This information is available free of charge via the Internet at http://pubs.acs.org/.

**REFERENCES**

(1) Patil, B. S.; Wang, Q.; Hessel, V.; Lang, J. Plasma N2-Fixation: 1900–2014. *Catalysis Today* **2015**, *256*, 49–66. https://doi.org/10.1016/j.cattod.2015.05.005.

(2) Patil, B. S.; Hessel, V.; Seefeldt, L. C.; Dean, D. R.; Hoffman, B. M.; Cook, B. J.; Murray, L. J. Nitrogen Fixation. In *Ullmann's Encyclopedia of Industrial Chemistry*; Wiley-VCH Verlag GmbH & Co. KGaA: Weinheim, Germany, 2017; pp 1–21. https://doi.org/10.1002/14356007.a17_471.pub2.

(3) Appl, M. Ammonia, 2. Production Processes. *Ullmann's encyclopedia of industrial*

*chemistry* **2012**, 139–225. https://doi.org/10.1002/14356007.o02.

(4) Appl, M. The Haber-Bosch Heritage: The Ammonia Production Technology. In *50th Anniversary of the IFA Technical Conference*; Sevilla, Spain, 1997; p 25.

(5) Smil, V. *Enriching the Earth: Fritz Haber, Carl Bosch, and the Transformation of World Food Production*; MIT Press, 2004.

(6) Anastasopoulou, A.; Butala, S.; Patil, B.; Suberu, J.; Fregene, M.; Lang, J.; Wang, Q.; Hessel, V. Techno-Economic Feasibility Study of Renewable Power Systems for a Small-Scale Plasma-Assisted Nitric Acid Plant in Africa. *Processes* **2016**, *4* (4), 54. https://doi.org/10.3390/pr4040054.

(7) Lan, R.; Irvine, J. T. S.; Tao, S. Ammonia and Related Chemicals as Potential Indirect Hydrogen Storage Materials. *International Journal of Hydrogen Energy* **2012**, *37* (2), 1482–1494. https://doi.org/10.1016/j.ijhydene.2011.10.004.

(8) Morgan, E.; Manwell, J.; McGowan, J. Wind-Powered Ammonia Fuel Production for Remote Islands: A Case Study. *Renewable Energy* **2014**, *72*, 51–61. https://doi.org/10.1016/j.renene.2014.06.034.

(9) Gieshoff, J.; Lang, J. Process For The Plasma-Catalytic Production of Ammonia. US6471932, 2002.

(10) Bramsiepe, C.; Sievers, S.; Seifert, T.; Stefanidis, G. D.; Vlachos, D. G.; Schnitzer, H.; Muster, B.; Brunner, C.; Sanders, J. P. M.; Bruins, M. E.; et al. Low-Cost Small Scale Processing Technologies for Production Applications in Various Environments — Mass Produced Factories. *Chemical Engineering & Processing: Process Intensification* **2012**, *51*, 32–52. https://doi.org/10.1016/j.cep.2011.08.005.

(11) Seifert, T.; Sievers, S.; Bramsiepe, C.; Schembecker, G. Small Scale , Modular and Continuous : A New Approach in Plant Design. *Chemical Engineering & Processing: Process Intensification* **2012**, *52*, 140–150. https://doi.org/10.1016/j.cep.2011.10.007.

(12) Patil, B. S.; Wang, Q.; Hessel, V.; Lang, J. Plasma Assisted Nitrogen Fixation Reactions. In *Alternative Energy Sources For Green Chemistry*; Stefanidis, G. D., Stankiewicz, A., Eds.; Royal Society of Chemistry: Cambridge, UK, 2016. https://doi.org/10.1039/9781782623632-00296.

(13) Hessel, V.; Cravotto, G.; Fitzpatrick, P.; Patil, B. S.; Lang, J.; Bonrath, W. Industrial Applications of Plasma , Microwave and Ultrasound Techniques : Nitrogen-Fixation and

Hydrogenation Reactions. *Chemical Engineering and Processing: Process Intensification* **2013**, *71*, 19–30. https://doi.org/10.1016/j.cep.2013.02.002.

(14) Nørskov, J.; Contacts, B.; Miranda, R.; Fitzsimmons, T.; Stack, R.; Singh, A.; Rohr, B.; University, S.; Goldstein, J. Sustainable Ammonia Synthesis Exploring the Scientific Challenges Associated with Discovering Alternative, Sustainable Processes for Ammonia Production DOE Roundtable Report SUSTAINABLE AMMONIA SYNTHESIS. **2016**.

(15) Samukawa, S.; Hori, M.; Rauf, S.; Tachibana, K.; Bruggeman, P.; Kroesen, G.; Whitehead, J. C.; Murphy, A. B.; Gutsol, A. F.; Starikovskaia, S.; et al. The 2012 Plasma Roadmap. *Journal of Physics D: Applied Physics* **2012**, *45* (25), 253001. https://doi.org/10.1088/0022-3727/45/25/253001.

(16) Ingels, R.; Graves, D.; Anderson, S.; Koller, R. Modern Plasma Technology for Nitrogen Fixation: New Opportunities? In *International Fertiliser Society*; International Fertiliser Society: London, UK, 2015; pp 1–27.

(17) Cherkasov, N.; Ibhadon, A. O.; Fitzpatrick, P. A Review of the Existing and Alternative Methods for Greener Nitrogen Fixation. *Chemical Engineering and Processing: Process Intensification* **2015**, *90*, 24–33. https://doi.org/10.1016/j.cep.2015.02.004.

(18) Patil, B. S.; Peeters, F. J. J.; Medrano, J. A.; van Rooij, G. J.; Gallucci, F.; Lang, J.; Wang, Q.; Hessel, V. Plasma Assisted Nitrogen Oxide Production from Air: Using Pulsed Powered Gliding Arc Reactor for a Containerized Plant. *AIChE Journal* **2018**, *64* (2), 526–537. https://doi.org/10.1002/aic.15922.

(19) Patil, B. S. Plasma (Catalyst) – Assisted Nitrogen Fixation : Reactor Development for Nitric Oxide and Ammonia Production, Eindhoven University of Technology, The Netherlands, 2017.

(20) Fridman, A. *Plasma Chemistry*; Cambridge University Press: New York, 2008.

(21) Lieberman, M. A.; Lichtenberg, A. J. *Principles of Plasma Discharges and Materials Processing*; Wiley, 2005.

(22) Stere, C. E.; Adress, W.; Burch, R.; Chansai, S.; Goguet, A.; Graham, W. G.; Rosa, F. De; Palma, V.; Hardacre, C. Ambient Temperature Hydrocarbon Selective Catalytic Reduction of NOx Using Atmospheric Pressure Nonthermal Plasma Activation of a Ag/Al2O3 Catalyst. *ACS Catalysis* **2014**, *4*, 666–673. https://doi.org/10.1021/cs4009286.

(23) Gómez-Ramírez, A.; Rico, V. J.; Cotrino, J.; González-Elipe, A. R.; Lambert, R. M. Low

Temperature Production of Formaldehyde from Carbon Dioxide and Ethane by Plasma-Assisted Catalysis in a Ferroelectrically Moderated Dielectric Barrier Discharge Reactor. *ACS Catalysis* **2014**, *4* (2), 402–408. https://doi.org/10.1021/cs4008528.

(24) Wang, L.; Yi, Y.; Zhao, Y.; Zhang, R.; Zhang, J.; Guo, H. NH3 Decomposition for H2 Generation: Effects of Cheap Metals and Supports on Plasma–Catalyst Synergy. *ACS Catalysis* **2015**, 4167–4174. https://doi.org/10.1021/acscatal.5b00728.

(25) Stere, C. E.; Adress, W.; Burch, R.; Chansai, S.; Goguet, a.; Graham, W. G.; Hardacre, C. Probing a Non-Thermal Plasma Activated Heterogeneously Catalyzed Reaction Using in Situ DRIFTS-MS. *ACS Catalysis* **2015**, *5* (2), 956–964. https://doi.org/10.1021/cs5019265.

(26) Whitehead, J. C. Plasma Catalysis: A Solution for Environmental Problems. *Pure and Applied Chemistry* **2010**, *82* (6), 1329–1336. https://doi.org/10.1351/PAC-CON-10-02-39.

(27) Zhang, Y. R.; Van Laer, K.; Neyts, E. C.; Bogaerts, A. Can Plasma Be Formed in Catalyst Pores? A Modeling Investigation. *Applied Catalysis B: Environmental* **2016**, *185*, 56–67. https://doi.org/10.1016/j.apcatb.2015.12.009.

(28) Bai, M.; Zhang, Z.; Bai, X.; Bai, M.; Ning, W. Plasma Synthesis of Ammonia with a Microgap Dielectric Barrier Discharge at Ambient Pressure. *IEEE Transactions on Plasma Science* **2003**, *31* (6), 1285–1291. https://doi.org/10.1109/TPS.2003.818761.

(29) Bai, M.; Zhang, Z.; Bai, M.; Bai, X.; Gao, H. Synthesis of Ammonia Using CH4/N2 Plasmas Based on Micro-Gap Discharge under Environmentally Friendly Condition. *Plasma Chemistry and Plasma Processing* **2008**, *28* (4), 405–414. https://doi.org/10.1007/s11090-008-9132-4.

(30) Mizushima, T.; Matsumoto, K.; Sugoh, J.; Ohkita, H.; Kakuta, N. Tubular Membrane-like Catalyst for Reactor with Dielectric-Barrier-Discharge Plasma and Its Performance in Ammonia Synthesis. *Applied Catalysis A: General* **2004**, *265* (1), 53–59. https://doi.org/10.1016/j.apcata.2004.01.002.

(31) Patil, B. S.; Peeters, F. J. J.; Kaathoven, A. S. R. van; V., H.; J., L.; Q., W. Deciphering the Plasma-Catalyst Support Interaction for Plasma Assisted Ammonia Synthesis in a Packed DBD Reactor. JPhysD: Applied Physics 2020, 53, 114001.

(32) Mingdong, B.; Xiyao, B.; Zhitao, Z. Synthesis of Ammonia in a Strong Electric Field Discharge at Ambient Pressure. *Plasma Chemistry and Plasma Processing* **2000**, *20* (4), 511–520.

(33) Hong, J.; Prawer, S.; Murphy, A. B. Production of Ammonia by Heterogeneous Catalysis in a Packed-Bed Dielectric-Barrier Discharge : Influence of Argon Addition and Voltage. *IEEE TRANSACTIONS ON PLASMA SCIENCE* **2014**, *42* (10), 2338–2339.

(34) Gómez-Ramírez, A.; Cotrino, J.; Lambert, R. M.; González-Elipe, A. R. Efficient Synthesis of Ammonia from N2 and H2 Alone in a Ferroelectric Packed-Bed DBD Reactor. *Plasma Sources Science and Technology* **2015**, *24* (6), 065011. https://doi.org/10.1088/0963-0252/24/6/065011.

(35) Gómez-Ramírez, A.; Montoro-Damas, A. M.; Cotrino, J.; Lambert, R. M.; González-Elipe, A. R. About the Enhancement of Chemical Yield during the Atmospheric Plasma Synthesis of Ammonia in a Ferroelectric Packed Bed Reactor. *Plasma Processes and Polymers* **2016**, No. August, 1–8. https://doi.org/10.1002/ppap.201600081.

(36) Patil, B. S.; Cherkasov, N.; Lang, J.; Ibhadon, A. O.; Hessel, V.; Wang, Q. Low Temperature Plasma-Catalytic NOx Synthesis in a Packed DBD Reactor: Effect of Support Materials and Supported Active Metal Oxides. *Applied Catalysis B: Environmental* **2016**, *194*, 123–133. https://doi.org/10.1016/j.apcatb.2016.04.055.

(37) Mizushima, T.; Matsumoto, K.; Ohkita, H.; Kakuta, N. Catalytic Effects of Metal-Loaded Membrane-like Alumina Tubes on Ammonia Synthesis in Atmospheric Pressure Plasma by Dielectric Barrier Discharge. *Plasma Chemistry and Plasma Processing* **2006**, *27* (1), 1–11. https://doi.org/10.1007/s11090-006-9034-2.

(38) Peng, P.; Li, Y.; Cheng, Y.; Deng, S.; Chen, P.; Ruan, R. Atmospheric Pressure Ammonia Synthesis Using Non-Thermal Plasma Assisted Catalysis. *Plasma Chemistry and Plasma Processing* **2016**, *36* (5), 1201–1210. https://doi.org/10.1007/s11090-016-9713-6.

(39) Hong, J.; Aramesh, M.; Shimoni, O.; Seo, D. H.; Yick, S.; Greig, A.; Charles, C.; Prawer, S.; Murphy, A. B. Plasma Catalytic Synthesis of Ammonia Using Functionalized-Carbon Coatings in an Atmospheric-Pressure Non-Equilibrium Discharge. *Plasma Chemistry and Plasma Processing* **2016**, *36*, 917–940. https://doi.org/10.1007/s11090-016-9711-8.

(40) Iwamoto, M.; Akiyama, M.; Aihara, K.; Deguchi, T. Ammonia Synthesis on Wool-Like Au, Pt, Pd, Ag, or Cu Electrode Catalysts in Nonthermal Atmospheric-Pressure Plasma of N2 and H2. *ACS Catalysis* **2017**, *7* (10), 6924–6929. https://doi.org/10.1021/acscatal.7b01624.

(41) Mehta, P.; Barboun, P.; Herrera, F. A.; Kim, J.; Rumbach, P.; Go, D. B.; Hicks, J. C.;

Schneider, W. F. Overcoming Ammonia Synthesis Scaling Relations with Plasma-Enabled Catalysis. *Nature Catalysis* **2018**, *1*, 269–275.

(42) Manley, T. C. The Electric Characteristics of the Ozonator Discharge. *Trans Electrochem. Soc* **1943**, *84*, 83–96. https://doi.org/10.1149/1.3071556.

(43) Sabat, K. C.; Rajput, P.; Paramguru, R. K.; Bhoi, B.; Mishra, B. K. Reduction of Oxide Minerals by Hydrogen Plasma: An Overview. *Plasma Chemistry and Plasma Processing* **2014**, *34* (1), 1–23. https://doi.org/10.1007/s11090-013-9484-2.

(44) Chen Laiyuan, Ni Yueqin, Zang Jingling, Lin Liwu, Luo Xihui, C. Sen. Structure Characterization of Platina/Alumina, Rhenium/Alumina, and Platinum-Rhenium/Alumina Catalysts. *Journal of Catalysis* **1993**, *145*, 132–140.

(45) H. F. J. van't Blik; J. B. A. D. van Zon; Huizinga, T.; Koningsberger, D. C.; Prins, R. Structure of Rhodium in an Ultradispersed Rh/Al2O3 Catalyst as Studied by EXAFS and Other Techniques. *Journal American Chemical Society* **1985**, *107* (11), 3139–3147.

(46) Gao, X.; Shen, J.; Hsias, Y.; Chen, Y. Reduction of Supported Iron Oxide Studied by Temperature-Programmed Reduction Combined with Mossbauer Spectroscopy and X-Ray Diffraction. *Journal of Chemical Society Faraday Transactions* **1993**, *89*, 1079–1084.

(47) Chiuping Li, Y.-W. C. Temperature-Programmed-Reduction Studies of Nickel Oxide / Alumina Catalysts : Effects of the Preparation Method. *Thermochimica Acta* **1995**, *256*, 457–465.

(48) Babu, N. S.; Lingaiah, N.; Gopinath, R.; Reddy, P. S. S.; Prasad, P. S. S. Characterization and Reactivity of Alumina-Supported Pd Catalysts for the Room-Temperature Hydrodechlorination of Chlorobenzene. *Journal of Physical Chemistry* **2007**, *111*, 6447–6453.

(49) V. Mazzieri, F. Coloma-Pascual, A. Arcoya, P.C. L'Argentiere, N. S. F. XPS , FTIR and TPR Characterization of Ru / Al2O3 Catalysts. *Applied Surface Science* **2003**, *210*, 222–230. https://doi.org/10.1016/S0169-4332(03)00146-6.

(50) Wang, H.; Liu, Z.; Wu, Y.; Yao, Z.; Zhao, W.; Duan, W. Preparation of Highly Dispersed W / Al 2 O 3 Hydrodesulfurization Catalysts via a Microwave Hydrothermal Method : Effect of Oxalic Acid. *Arabian Journal of Chemistry* **2016**, *9* (1), 18–24. https://doi.org/10.1016/j.arabjc.2014.11.023.

(51) Freek Kapteijn, A. Dick van Langeveld, J. A. M. Alumina-Supported Manganese Oxide

Catalysts. *Journal Of Catalysis* **1994**, No. 150, 94–104.

(52) Brown, R.; Cooper, E.; Whan, D. A. Temperature Programmed Reduction of Alumina-Supported Iron, Cobalt, and Nickel Bimetallic Catalysts. *Applied Catalysis* **1982**, *3*, 177–186.

(53) Frost, D. C.; McDowell, C. A. The Dissociation Energy of the Nitrogen Moolecule. *Royal Society of London. Mathematical and physical sciences* **1956**, *A*, 278–284.

(54) Herzberg, G. The Dissociation Energy of the Hydrogen Molecule. *J. Mol. Spectrosc.* **1970**, *33* (1), 147–168. https://doi.org/10.1016/0022-2852(70)90060-3.

(55) Roland, U.; Holzer, F.; Kopinke, F. Improved Oxidation of Air Pollutants in a Non-Thermal Plasma. *Catalysis Today* **2002**, *73*, 315–323.

(56) Zhang, Q.-Z.; Wang, W.-Z.; Bogaerts, A. Importance of Surface Charging during Plasma Streamer Propagation in Catalyst Pores. *Plasma Sources Science and Technology* **2018**, *27* (6).

(57) Jacobsen, C. J. H.; Dahl, S.; Boisen, A.; Clausen, B. S.; Topsøe, H.; Logadottir, A.; Nørskov, J. K. Optimal Catalyst Curves: Connecting Density Functional Theory Calculations with Industrial Reactor Design and Catalyst Selection. *Journal of Catalysis* **2002**, *205* (2), 382–387. https://doi.org/http://dx.doi.org/10.1006/jcat.2001.3442.

(58) Medford, A. J.; Vojvodic, A.; Hummelshøj, J. S.; Voss, J.; Abild-Pedersen, F.; Studt, F.; Bligaard, T.; Nilsson, A.; Nørskov, J. K. From the Sabatier Principle to a Predictive Theory of Transition-Metal Heterogeneous Catalysis. *Journal of Catalysis* **2015**, *328*, 36–42. https://doi.org/https://doi.org/10.1016/j.jcat.2014.12.033.

(59) Madix, R. J.; Benziger, J. Kinetic Processes on Metal Single-Crystal Surfaces. *Annual review of physical chemistry* **1978**, *29*, 285–306.

(60) Peeters, F. J. J.; Yang, R.; van de Sanden, M. C. M. The Relation between the Production Efficiency of Nitrogen Atoms and the Electrical Characteristics of a Dielectric Barrier Discharge. *Plasma Sources Science and Technology* **2015**, *24* (4), 045006. https://doi.org/10.1088/0963-0252/24/4/045006.

(61) Sharma, M. K.; Saikia, B. K. Discharge Conditions and Emission Spectroscopy of N2 and N 2+ Active Species in a Variable Power Dc Pulsed Plasma Used for Steel Nitriding. *Indian Journal of Pure and Applied Physics* **2008**, *46* (7), 463–470.

(62) Petitjean, L.; Ricard, A. Emission Spectroscopy Study of N2-H2 Glow Discharge for Metal

Surface Nitriding. *Journal of Physics D: Applied Physics* **1984**, *17*, 919–929.

(63) Camacho, J. J.; Poyato, J. M. L.; Díaz, L.; Santos, M. Optical Emission Studies of Nitrogen Plasma Generated by IR CO2laser Pulses. *Journal of Physics B: Atomic, Molecular and Optical Physics* **2007**, *40* (24), 4573–4590. https://doi.org/10.1088/0953-4075/40/24/003.

(64) Zhang, Q. Y.; Shi, D. Q.; Xu, W.; Miao, C. Y.; Ma, C. Y.; Ren, C. S.; Zhang, C.; Yi, Z. Determination of Vibrational and Rotational Temperatures in Highly Constricted Nitrogen Plasmas by Fitting the Second Positive System of N2 Molecules. *AIP Advances* **2015**, *5* (057158), 1–11. https://doi.org/10.1063/1.4921916.

(65) Hong, J.; Prawer, S.; Murphy, A. B. Plasma Catalysis as an Alternative Route for Ammonia Production: Status, Mechanisms, and Prospects for Progress. *ACS Sustainable Chemistry & Engineering* **2018**, *6*, 15–31. https://doi.org/10.1021/acssuschemeng.7b02381.

(66) Hong, J.; Pancheshnyi, S.; Tam, E.; Lowke, J. J. Kinetic Modelling of NH 3 Production in N 2 – H 2 Non-Equilibrium Atmospheric-Pressure Plasma Catalysis. *Journal of Physics D: Applied Physics* **2017**, *50* (154005), 1–33.

(67) Nakajima, J.; Sekiguchi, H. Synthesis of Ammonia Using Microwave Discharge at Atmospheric Pressure. *Thin Solid Films* **2008**, *516* (13), 4446–4451. https://doi.org/10.1016/j.tsf.2007.10.053.

(68) Yin, K. S.; Venugopalan, M. Plasma Chemical Synthesis. I. Effect of Electrode Material on the Synthesis of Ammonia. *Plasma Chemistry and Plasma Processing* **1983**, *3* (3), 343–350.

(69) Kiyooka, H.; Matsumoto, O. Reaction Scheme of Ammonia Synthesis in the ECR Plasmas. *Plasma Chemistry and Plasma Processing* **1996**, *16* (4), 547–562.

(70) Patil, B. S.; Peeters, F. J. J.; Kaathoven, A. S. R. van; V., H.; J., L.; Q., W. Deciphering the Plasma-Catalyst Support Interaction for Plasma Assisted Ammonia Synthesis in a Packed DBD Reactor. JPhysD: Applied Physics 2020, 53, 114001.